Optics & Laser Technology 161 (2023) 109158

Contents lists available at ScienceDirect

Optics and Laser Technology

journal homepage: www.elsevier.com/locate/optlastec

Full length article

Selective distributed optical fiber sensing system based on silicone cladding optical fiber and Rayleigh backscattering reflectometry for the detection of hydrocarbon leakages

Andrea Baggio [a], Matteo Turani [a,c], Massimo Olivero [b,*], Milena Salvo [a], Diego Pugliese [a,b], Marco Sangermano [a]

[a] Dipartimento di Scienza Applicata e Tecnologia (DISAT), Politecnico di Torino, Torino 10129, Italy
[b] Dipartimento di Elettronica e Telecomunicazioni (DET), Politecnico di Torino, Torino 10129, Italy
[c] Inspire AG, St. Gallen CH-9014, Switzerland

ARTICLE INFO

Keywords:
Optical fiber sensing
Chemical sensing
Hydrocarbon detection
Optical time domain reflectometry
Optical frequency domain reflectometry

ABSTRACT

A new system that exploits optical fiber distributed sensing for the detection of hydrocarbons is presented. The system relies on a custom-designed silica core/thin silicone cladding optical fiber to provide a quick and selective absorption of oil products through the cladding; moreover, it exhibits insensitivity to water. Optical fiber sensor interrogation is performed by detecting Rayleigh backscattering using an optical time domain reflectometer or, in a high-resolution version, an optical frequency domain reflectometer. The Rayleigh backscattering signal is influenced by a change in the refractive index of the cladding, which locally modifies the guiding properties of the fiber; and by the swelling of the cladding, resulting from hydrocarbon diffusion, that produces local stress and results in an associated increased reflection. The system has been tested with different solvents and has exhibited selectivity and a rapid response to exposure to high refractive index hydrocarbons, with the sensing fiber yielding a response time of the order of 1 s. The system, in its high-resolution version, is able to accurately locate leakages with an accuracy of 14 cm.

1. Introduction

The world's production capacity of petrochemicals is expected to grow by 50 % between 2020 and 2030 [1]. Therefore, the control of undesired releases of oil products into the environment constitutes a key issue, for both economic and environmental reasons [2,3].

A reliable, accurate and efficient monitoring system for the early detection of leakages is therefore necessary for storage and distribution sites. Since these sites are often exposed to the elements, leakages are likely to appear in water solutions, thus such a monitoring system should also be able to detect even very low concentrations of oil products and be unaffected by humidity and/or water.

A number of optical techniques are currently available for the detection of hydrocarbon (HC) concentrations in water solutions, such as gas chromatography-flame ionization detectors [4], gas chromatography-mass spectroscopy [5], and infrared [6], ultraviolet (UV) [7], Raman [8], and fluorescence [9] spectrometry. All of these techniques ensure an accurate measurement of HC concentrations in water solutions. However, they all suffer from the major disadvantage of needing to be performed in a laboratory and of not being suitable for in situ work or in real-time.

Indeed, the real-time feature is required in primary oil storage facilities where several tanks containing oil products (e.g., petrol, diesel, jet fuel) are installed over an area of several hectares, and where the prompt detection of leakages is crucial. These tanks may have a diameter of 60 to 100 m and are normally built with a double bottom. The bottom is made of welded steel sheets and the most likely defects that lead to leakages are cracks along the welding lines or pinholes caused by corrosion. The most suitable arrangement to monitor the leakages of these tanks is a sensor grid on the bottom liner, which may also be in the form of a sensing cable positioned in a kind of Greek fret.

Commercial monitoring systems, based on electrical detection, that

Abbreviations: HC, hydrocarbon; UV, ultraviolet; OTDR, optical time domain reflectometry/reflectometer; OFDR, optical frequency domain reflectometry/reflectometer; RI, refractive index; NA, numerical aperture.

* Corresponding author at: Department of Electronics and Telecommunications, Politecnico di Torino, c.so Duca degli Abruzzi 24, 10129 Torino, Italy.
E-mail address: massimo.olivero@polito.it (M. Olivero).

https://doi.org/10.1016/j.optlastec.2023.109158
Received 2 September 2022; Received in revised form 12 December 2022; Accepted 9 January 2023
Available online 20 January 2023

exploit this concept have been developed [10]. Optical fibers are one of the most interesting technologies in this field, since they may be tailored to perform the same previously mentioned task, but can offer other important advantages, such as an inherent fire safety (no electrical signals are carried by the optical fiber), smaller form factor and the possibility of monitoring longer distances.

R. Falate *et al.* [11] reported an interesting alternative for the chemical detection of HCs using long-period gratings inscribed in optical fibers. Although this method is effective in terms of sensitivity, it requires the implementation of a spot measurement and an extra processing of the fiber to inscribe the sensitive, long-period grating. The desired sensing platform should be distributed, i.e., the fiber should itself work as a sensor along its entire length [12]. Optical fiber distributed sensing systems are often used, through an indirect measurement, to detect chemicals, e.g., from mechanical stress on the fiber due to swelling after the absorption/adsorption of liquids [13,14], optical acoustic sensing [15], or changes in temperature [16]. Optical fiber acoustic sensing, relying on Brillouin scattering, as well as optical fiber temperature sensing, based on distributed measurement of Raman scattering, have been extensively used in leakage detection of pipelines, in which mechanical and thermal signatures can be correlated to leakages. For instance, a reference publication by Nikles [17] reports on a commercial pipeline integrity monitoring system that addresses the detection of a number of threats (leakage, permafrost, intrusion…) by temperature and strain measurement, exploiting Brillouin scattering. Acoustic sensing has also been implemented by measuring mechanical vibrations through the Rayleigh backscattering signature using Coherent Optical Time Domain Reflectometry (C-OTDR) [18]. Yet, a chemical-induced strain can be detected on a standard optical fiber coated with an oleophilic elastomer, by measuring the change of Rayleigh backscattering with Optical Frequency Domain Reflectometry (OFDR) [14]. Although the presented works, based on the measurement of mechanical and thermal features, have demonstrated to be effective in monitoring pipelines, the detection of leakages in storage tanks is more challenging and operators demand for a system that can selectively detect leakages of HCs, even when they are dissolved in water, with a high confidence and minimum likelihood of false alarms [19].

E. Sensfelder *et al.* [20] were the first to develop a silicone cladding optical fiber system which was able to detect pure chlorinated HCs in a water solution by means of the selective absorption of these chemicals rather than water. Buerck *et al.* then investigated and tested a similar system using different species of HCs [21,22] considering a 200 μm diameter optical fiber and a cladding thickness of 100 μm. In these systems, when the absorbed phase (e.g., an HC) has a different refractive index (RI) from the cladding of the sensing fiber, the RI of the cladding changes locally. Thus, the optical properties of the optical fiber are altered as is the carried signal. Whenever the RI of silicone cladding increases, due to the absorption of HCs, the numerical aperture (NA) of the fiber decreases. As a consequence, a number of guided modes in the fiber become radiating modes, and part of the propagating signal is lost locally.

An Optical Time Domain Reflectometer (OTDR) is particularly suitable to detect and localize signal losses through the fiber [23,24]. OTDRs are traditionally used in optical communication networks, but thanks to their usability, portability, and low cost, they have also found applications in sensing systems.

The optical fiber sensing system here proposed for the detection of HC leakages, which focuses on oil storage tanks, exploits the previously introduced concepts and is based on the measurement of Rayleigh backscattering from a silicone cladding optical fiber by means of an OTDR, according to the scheme shown in Fig. 1. In an OTDR, a laser diode launches an optical pulse into the sensing fiber; the backscattered signal is separated from the input pulse by a coupler and first converted into an electrical signal, by a photodetector, and then into digital information by means of analog-to-digital conversion and is displayed as a function of its position along the fiber. The inherent Rayleigh

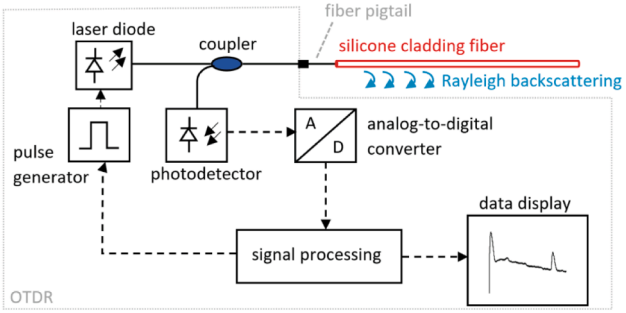

Fig. 1. Schematic of the OTDR setup for HC detection, including the operating principle of the OTDR. The dashed arrows represent electrical connections, whereas the solid lines indicate the path of the optical signal.

backscattering signal depends on the structure of the glass and on the presence of defects along the fiber. Under standard operating conditions, this signal appears to decrease as a function of length because of the inherent loss of the fiber, and may show down-steps, corresponding to localized losses, or spikes, which stem from concentrated reflections. In this application, the diffusion of HCs through the cladding produces a localized loss, due to changes in the RI of the cladding and subsequent changes in the guiding properties, as well as mechanical stress due to swelling.

The main novelty of the system presented here is that it relies on the use of a thin, custom-designed optical fiber with a silicone cladding that is selectively sensitive to HCs. Although the overall setup is similar to that presented in [18], this system exploits a fiber that has been designed with a reduced cladding thickness to obtain a prompt response (within a second) to HCs. The response time is experimentally evaluated by means of a simple transmission test. The fiber also exhibits a core/cladding structure that can efficiently be pigtailed and connected to standard OTDRs. Since its application may require a centimetric accuracy identification of a leakage, the silicone cladding fiber has also been tested with OFDR [25], which appears to be a more accurate alternative to OTDR. The work presented by Totland *et al.* [14] may resemble this approach, but in that case a polyamide-coated optical fiber was upgraded with a swelling elastomer coating to produce a mechanical strain when exposed to decane oil; besides the difference in the structure of the fiber, this sensing system exhibited full response to HC exposure within minutes. To the best of the authors' knowledge, this is the first demonstration of the combined use of silicone cladding optical fibers with OFDR for the high spatial resolution detection of HCs. The remaining part of the paper is organized in two sections, the first of which reports the materials and methods used to characterize the system, while the second reports the results of the measurements.

2. Materials and methods

2.1. Experimental investigation of the hydrophobic cladding material and fiber fabrication

In order to develop an optical fiber that is sensitive to HCs, but also exhibits negligible sensitivity to the effect of water, a suitable silicone was applied as the cladding material of the sensing optical fiber. In this case, the chosen polymer was a UV-curable silicone EFIRON FSC-440H type (Fospia, South Korea). This silicone was specifically designed for cladding or for the coating of silica optical fibers, since it presents high oxidative and hydrolytic stability. The RI of the cured polymer is 1.440 at 850 nm. Since the RI of pure silica is 1.453 at the same wavelength [26], the resulting NA of the fabricated fiber is equal to 0.194.

The performance of this silicone for the selective detection of HCs was experimentally investigated by measuring the absorption of both water and the main HCs of interest in bulk samples. The study was

carried out by conducting gravimetric tests on cured 2.35 ± 0.50 mm thick silicone blocks, following the procedure described hereafter. The silicone samples were produced by means of a standard lab. procedure: the resin was poured into a mold and cured for 30 s by a Lightning Cure LC8 UV lamp (Hamamatsu), whose UV beam is delivered through a flexible lightpipe. The silicone blocks were then extracted from the mold and the other side was exposed to UV light to obtain a uniform curing of the specimen. Several pristine samples were tested by immersing them in distilled water, xylene, dodecane, toluene, chloroform, and acetone. These samples were subjected to diffusion at increasing time steps, and the weight was recorded, at each step, with an analytical scale at 0.1 mg of resolution. The diffusion tests were carried out for up to 24 h, and the weight was recorded even after pulling out the samples from the baths, to establish the presence of any possible in-air desorption. The gravimetric values were used to estimate the diffusion coefficient (D) of each solvent in the silicone, through an approximate 1-dimensional (1-D) diffusion model [27], using Eq. (1):

$$D = \pi\left(\frac{h}{4M_\infty}\right)^2\left(\frac{M_2 - M_1}{\sqrt{t_2} - \sqrt{t_1}}\right)^2, \quad (1)$$

where h is the sample thickness, M_∞ is the weight gain measured at saturation, and M_2 and M_1 are the weight gains at the corresponding t_2 e t_1 times. The diffusion time (t) necessary for the solvent to penetrate the cladding to the depth of the core interface was then estimated, through Fick's law, by Eq. (2):

$$t = \frac{d^2}{4D}, \quad (2)$$

where t is the time that the solvent takes to diffuse through cladding thickness d, considering a diffusion coefficient D.

Apart from measuring the diffusion of the HCs in the silicone, a coarse assessment of the optical properties was performed, as a function of diffusion, by measuring the RI of the bulk silicone samples with a prism-coupling refractometer (Metricon 2010/M, USA). Fig. 2 reports the RI at various wavelengths (633, 825, 1061, 1312 and 1533 nm) of a silicone sample subjected to xylene diffusion for different time intervals. The data well reproduce Sellmeier's relationship of transparent media, with a decreasing RI for increased wavelengths. The graph also reports the RI values for silica glass, as reported in ref. [26]. When the sample undergoes diffusion for up to 60 min, the RI curve nearly reaches that of silica, thus indicating that an optical fiber structure with silicone cladding and a silica core would not fulfill the guiding condition, based on total internal reflection (i.e., RI of the core > RI of the cladding).

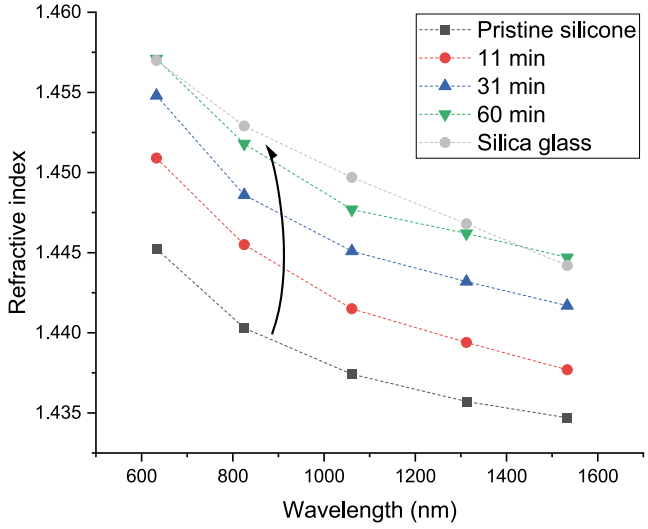

Fig. 2. RI values of the bulk silicone samples *vs* the wavelength for different immersion times in xylene. The arrow shows that the RI increases to the value of pure silica (the RI of silica was retrieved from [26]), the dashed lines are just indicated for readability purposes. This is a qualitative proof that a silica core/silicone cladding optical fiber can sense the diffusion of xylene through a change in its guiding properties.

Since the selective absorption of the bulk silicone had already been experimentally verified, a remarkable change in RI had been assessed and a diffusion time for quick detection of HCs had been devised, three different silicone cladding optical fibers were then designed and fabricated by Flexilicate ltd., Malaysia. Maintaining a core diameter of 50 ± 1 μm, which matches the dimension of the OTDR input, cladding thicknesses of 20, 30 and 40 μm were devised, thus resulting in fiber diameters of 90, 110 and 130 μm. As a result of fabrication tolerances, the drawn optical fibers had actual dimensions of 55 μm for the core diameter and 80, 100 and 120 μm for the overall fiber diameters. Because of their dimensions and the RI of the core/cladding structure, these fibers are strongly multimode at the wavelengths of interest, that are, of 850 nm (for OTDR interrogation) and 1550 nm (for OFDR interrogation). The V-number, the so-called normalized frequency that determines the number of supported modes, is defined by Eq. (3):

$$V = \frac{2\pi}{\lambda} \bullet r \bullet NA \quad (3)$$

where λ is the wavelength of interest, r is the core radius and NA is the numerical aperture ($NA = \sqrt{RI_{core}^2 - RI_{cladding}^2}$). In this case, $V = 39.4$ at 850 nm, thus resulting in a large number of supported modes M:

$$M = \frac{V^2}{2} \approx 776 \quad (4)$$

The diffusion of HCs with a higher RI than the cladding produces an increment of the cladding RI, which in turn reduces the number of guided modes and produces a local loss along the exposed fiber section, and this in turn can be detected by the OTDR. Proof-of-concept RI measurements on bulk samples, subjected to the long-term diffusion of xylene, resulted in an 0.011 increment of the silicone RI, which exceeded the RI of the core and nullified the total internal reflection of the fiber, i.e., $RI_{core} < RI_{cladding}$. An optical effect is also produced by the swelling of HCs, which induces a local stress that appears as a peak in the back-reflected signal.

2.2. Connectorization of the silicone fibers and testing

The fibers described above were cut into lengths of up to 50 m and fusion spliced with an optical fiber pigtail for telecommunications (multimode 62.5/125 μm with an FC-PC connector). The operation was performed by a fiber optic splicer FSM-90S model (Fujikura ltd., Japan), using a custom-developed recipe. A short section of the silicone cladding was mechanically stripped at the tip of the sensing fiber prior to splicing. The pigtail and the uncladded tip were fused together with the splicer electric arc, which was applied asymmetrically, i.e., close to the tip of the pigtail. This procedure was necessary because the diameter of the uncladded fiber was larger than that of the pigtail, thus a greater amount of energy had to be deposited onto the latter to melt it. The two tips were fused together by applying an arc of 1500 s and setting the power at 20 bits. A second arc with the same power and a duration of 900 ms was then triggered to taper the joint and produce a limited loss and mechanically sturdy connection. Finally, the joint was re-coated with silicone to restore the core-cladding structure. Fig. 3 reports three micrographs depicting the different splicing steps.

2.3. OTDR and OFDR measurements

The connectorized silicone cladding fiber was monitored by means of a VIAVI MTS 2000 OTDR model (VIAVI Solutions Inc., USA). The instrument emits laser pulses at a wavelength of 850 nm. It is worth noting that the choice of using an OTDR at 850 nm stems from the fact that

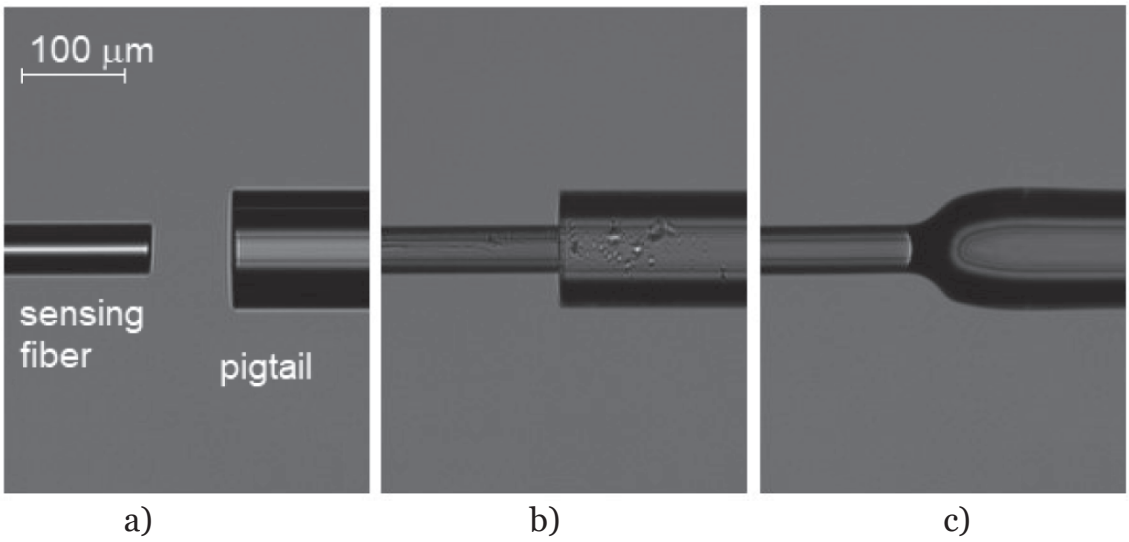

Fig. 3. Splicing between the silicone cladding sensing fiber (left) and the multimode fiber pigtail (right). Notice that the silicone cladding was removed and only the 55 μm core is present at the splicing interface. (a) Alignment of the fibers, (b) joint after the first fusion arc and (c) after the second arc.

Rayleigh backscattering inversely scales with the fourth power of the wavelength, thus leading to a signal on the OTDR that is about 1.6 times higher at this wavelength than that measured at a standard telecom wavelength of around 1550 nm. The pulse duration was set at the lowest value of 3 ns for this instrument to allow for the highest spatial resolution of 0.8 m. The acquisition time, set at 10 s for all the measurements, is the lowest value allowed by this instrument and it permits the scanning of a fiber length of up to 2 km. Most of the detection tests were performed on 30 m-long sensing fibers, although the sensing range is only limited by the fiber propagation loss and the detection capability.

The optical fibers were tested by wetting ca. 3 cm with pure HCs or by immersing a portion of ca. 30 cm in a crystallizer filled with a water solution of HCs at different concentrations. The used HCs were xylene (Sigma-Aldrich, purity $\geq$ 98.5 %), dodecane (Fluka Chemicals, purity $\geq$ 90 %), toluene (Sigma-Aldrich, purity $\geq$ 99.5 %), chloroform (Sigma-Aldrich, purity $\geq$ 99.5 %), and acetone (Sigma-Aldrich, purity $\geq$ 99.5 %).

Similar tests were also conducted by connecting the sensing fibers to an OBR4600 OFDR model (Luna Technologies, USA). It is here useful to recall the main features of an OFDR and its advantages for sensing applications, although comprehensive literature is available elsewhere.

The principle of operation of an OFDR may be better explained through the schematic diagram reported in Fig. 4.

OFDR instruments rely on a swept-wavelength laser coupled with a modified Mach-Zender interferometer. One leg of the interferometer is a reference path of fixed length, while the other leg is the tested optical fiber, being interrogated in reflection mode through a directional coupler. The backscattered light is combined with the light from the reference arm to generate an interference signal that contains information related to the accurate location (i.e., with sub-mm resolution) and magnitude of reflective events along the fiber length. An acquisition system collects a large number of intensity signals from the detector, as a function of the wavelength and time (by performing multiple sweeps). The intensity patterns are cross-correlated and, from the cross-correlation function (or better, its Fourier transform), it is possible to retrieve the complete spectral response (in terms of both real and imaginary parts) at any position along the tested fiber. Thus, the OFDR is able to measure the precise location of very small absorptions or reflective events along the tested fiber. In short, the basic signal yielded by the OFDR is, in the same way as for the OTDR, the Rayleigh backscattering from the fiber as a function of position, which exhibits drops or spikes corresponding to local modifications of the guiding properties due to external perturbations. The resolution of OTDR is of the order of 1 m, whereas the OFDR is capable of detecting perturbations far below 1 cm, which may be of great advantage for leakage detection purposes. Another advantage of the OFDR is that it does not exhibit a "dead zone", i.e., it can measure loss or reflective events very close to the input of the sensing fiber, whereas the OTDR cannot measure events in the first few meters of the fiber being tested (the "dead zone" depends on the instrument settings and the characteristics of the tested fiber).

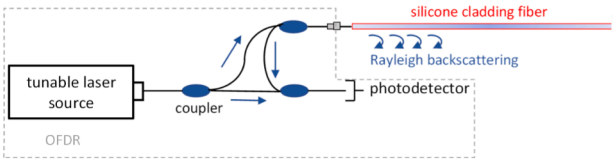

Fig. 4. Operating principle of Optical Frequency Domain Reflectometry (OFDR) (the black arrows indicate the path of the optical signal produced by the tunable laser).

In the case of OFDR testing, a single drop of pure solvent was placed onto the fiber cladding so that it would wet the fiber for a length of about 2 cm, in order to assess the achievable spatial resolution of the sensing system.

2.4. Time response

In order to assess the performance of the three different fiber designs (80, 100, and 120 μm cladding diameters, respectively), the time response to HC diffusion was investigated. For this measurement, the fiber under test was connected to a laser source (in this case, the internal laser of the OTDR was exploited) on one side, and to a high-speed photodetector (DET01CFC model, Thorlabs, USA) on the other side, by means of double pigtailing. The 850 nm wavelength laser signal was analyzed by an oscilloscope connected to the photodetector (a schematic representation of the complete measuring system is reported in Fig. 5). The laser was run in continuous wave mode, and a constant signal was therefore displayed by the oscilloscope under steady state conditions. A drop of xylene was placed onto the sensing fiber and the perturbation of the transmitted light was then registered.

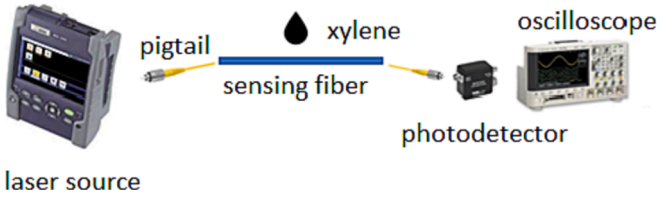

Fig. 5. Time response measurement of the silicone cladding fibers. The decrease in the transmitted optical signal, when the fiber is dipped in xylene, is detected by a photodiode and displayed on the oscilloscope.

3. Results and discussion

The gravimetric analysis clearly showed the selectivity of the cladding material in absorbing HCs. As shown in Fig. 6a, the weight of the silicone samples increased when they were immersed in organic solvents until saturation was reached. Conversely, when the cladding material was immersed in pure water, no change in weight was observed. Desorption of the HCs was also observed, as can be seen in Fig. 6b. The collected data were used to estimate, by means of Eq. (1), the diffusion coefficient of each HC. The approximate diffusion coefficients, of the order of 10^{-10} m^2/s, would result in a lower time, inof the order of a second, for the HCs to reach the core-cladding interface, as calculated by Eq. (2) and reported in Table 1. These values represent an estimation of the response time of the detecting system necessary to locate a leakage.

The actual detection capabilities of the system were first tested using pure solvents. A few drops of each chemical were placed onto a specific segment of the sensing fiber so that around 3 cm of the cladding was wetted. As theoretically predicted, when the cladding absorbed an HC with a higher RI than its own (xylene, toluene, and chloroform), the signal collected by the OTDR dropped, as shown by the traces reported in Fig. 7d-f. The peak at the furthest position along the fiber, which is produced by the glass-to-air reflection at the end of the fiber tip, should be noted. The detection tests conducted with low RI HCs (acetone and dodecane) and water did not show any signal perturbation. In the case of water, gravimetric analysis had previously demonstrated that water does not even diffuse through the cladding. HCs with a lower RI than that of the silicone cladding, although able to diffuse, did not change the guiding properties of the fiber, or produce a significant stress due to swelling that could be detected by OTDR. The relationship between the RI of the absorbed HC and the amount of the decrease in the OTDR signal also appears evident: for example, chloroform has the lowest RI, and it showed the lowest decrease. The actual decrease amounts are not measurable for xylene and toluene because the signal became lower than the −10 dB background noise of the instrument, whereas, in the case of chloroform (Fig. 7f), the down-step is of about 6 dB. In this case, the background noise of the OTDR was not reached, as the reflection peak from the end of the fiber tip remained observable after exposure to chloroform. It should be pointed out that the tests were repeated for all the fiber designs and the same behavior was observed for all the cladding thicknesses. Hence, the time response versus cladding thickness was only tested for xylene, since it was considered as the most representative of the HCs in real applications. The time response yielded values lower than 1 s and a nearly linear dependence on the cladding thickness (Fig. 8). The actual times taken by the optical signal to decrease, as reported in Fig. 8a, are shorter than those evaluated using Fick's law (Table 1), but are in good agreement, since the theoretical calculation does not take into account the cylindrical geometry of the optical fiber. It should be pointed out that the here reported response time values are more than one order of magnitude lower than those reported in similar works [21], thanks to the limited thickness of the silicone cladding.

Table 1
Diffusion coefficient of different HCs in the silicone cladding fibers and estimation of the response time of the sensing system based on Fick's low.

	Diffusion coefficient [m^2/s]	Expected time of diffusion from the cladding surface to the core-cladding interface [ms]		
		Fiber 1 diameter 80 μm/ cladding thickness 12.5 μm	Fiber 2 diameter 100 μm/ cladding thickness 22.5 μm	Fiber 3 diameter 120 μm/ cladding thickness 32.5 μm
xylene	1.7×10^{-10}	230	740	1550
dodecane	7.8×10^{-11}	500	1620	3390
toluene	2.4×10^{-10}	160	530	1100
chloroform	2.6×10^{-10}	150	490	1020
acetone	2.6×10^{-10}	150	490	1020

Desorption of HCs by the silicone cladding fibers, hence the reversibility of their response, was also investigated. The OTDR traces (Fig. 8d-f) nearly recovered to the original signatures when the fiber previously exposed to HCs was dried with a paper towel, confirming the results of the gravimetric tests.

The system was also tested with high RI HCs in a water solution to assess the detection limit. These tests were carried out with the 100 μm cladding fiber, which best matches a trade-off between mechanical stability and a quick response to HC exposure. Different concentrations were prepared, starting from the solubility limit of each HC, and gradually increasing the water content. A similar response to the pure HCs was observed when dipping about 30 cm of sensing fiber into the water solution. When the HC concentration was decreased, the drop decreased accordingly, until the limit of detection was reached. Fig. 9 reports the

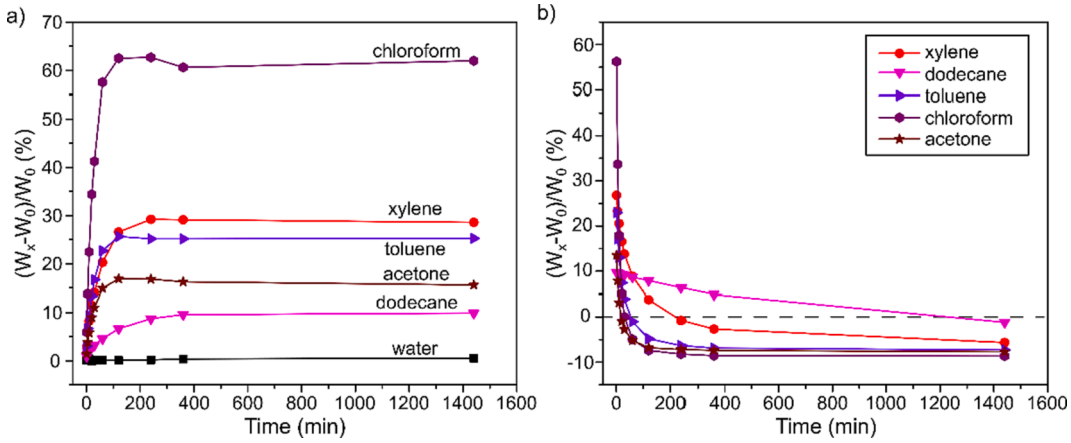

Fig. 6. Weight change in percentage during the a) absorption and b) desorption gravimetric tests using water, xylene, dodecane, toluene, chloroform, and acetone.

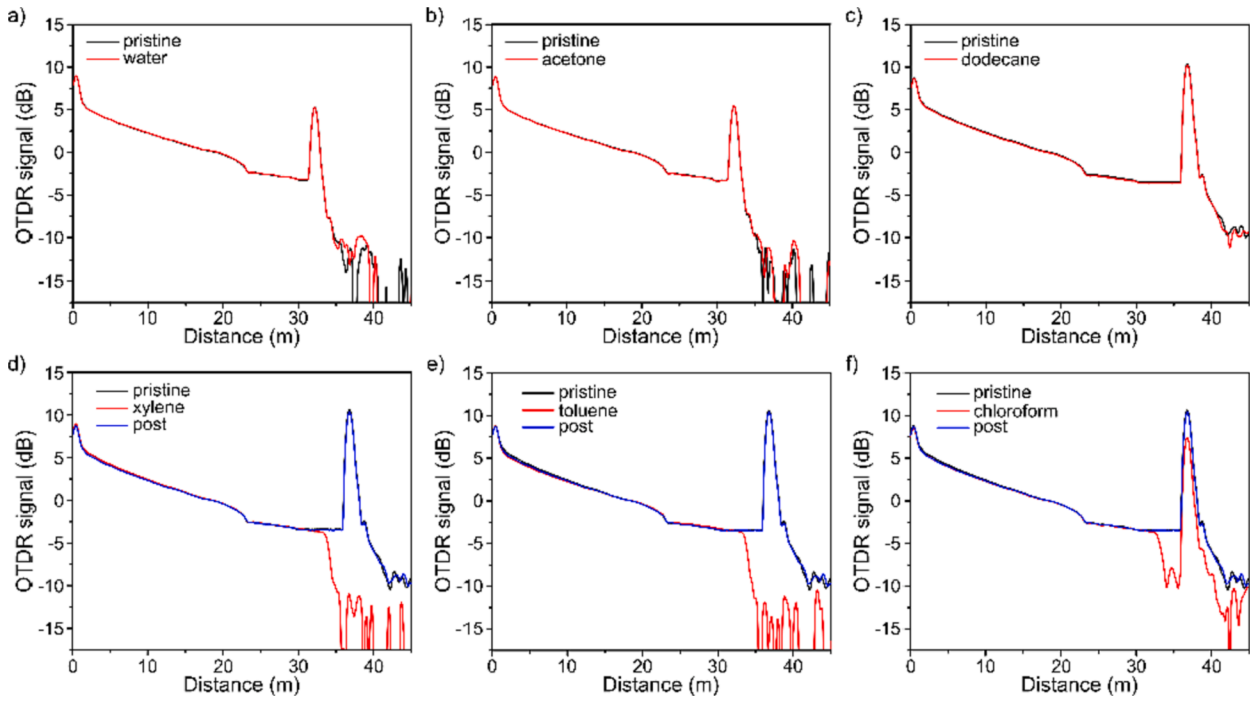

Fig. 7. Comparison of traces collected by OTDR before and after immersion, at a ~ 35 m position from the connector, of a 3 cm-long 100 μm diameter segment of silicone cladding fiber in: (a) water, (b) acetone, (c) dodecane, (d) xylene, (e) toluene, and (f) chloroform. The graphs d) to f) also report the OTDR trace after recovery of the sensing fiber from exposure to HCs.

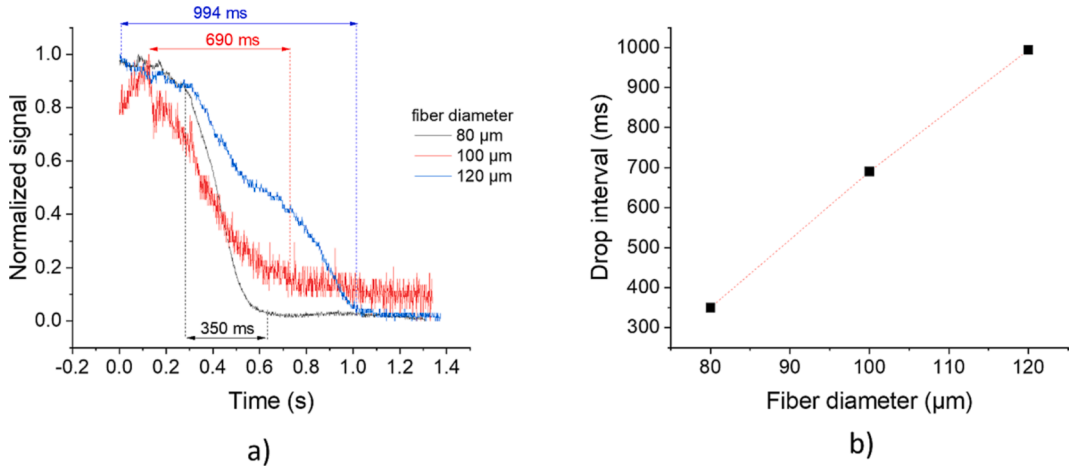

Fig. 8. Response time of the three types of fibers with different silicone cladding diameters tested with xylene: a) measured signal, normalized on a 0–1 scale and with indication of the response times, b) response time reported as a function of the cladding diameter.

OTDR traces of the responsive HCs at the detection limit, along with traces of the pristine fiber, i.e., collected before immersion in the HC solution. The results show a limit of detection of 25 mg/L (or ppm) for xylene, 350 mg/L for toluene, and 5500 mg/L for chloroform.

The possibility to detect multiple leakages with the sensing fiber is strictly related to the dynamics of the interrogation system and the response of the sensing fiber to the HC, that is, its type and concentration. In a real application it is expected that the leakage shows up as solution of HCs in water, so that the drop of the OTDR trace may not reach its noise floor. In that case, even multiple leakages can be detected. In our system the dynamic range of the OTDR is limited to 20 dB by the pulse width and the integration time, but depending on the specific application and measurement constraints (i.e., resolution and sampling time), this value may be increased. A proof-of-concept experiment was performed by testing the sensing fiber with dichloromethane that had a RI close to that of the silicone cladding and only produced a ~ 1.5 dB drop in the OTDR signature. Fig. 10 reports the change of the trace when the sensing fiber is exposed to dichloromethane in either one or two subsequent sections, showing that the two events are detectable.

The measurements performed with OTDR demonstrate a proof-of-concept of the technological platform for the selective and distributed detection of HCs based on fibers with a thin silicone cladding. The accuracy on the identification of the position along the fiber is determined by the measurement settings of the OTDR (pulse duration, duration of the measurement, signal strength, etc.), and it is also influenced by the maximum length of the measurement and the characteristics of the sensing fiber. The sensitivity of the OTDR used here, but in general of this type of instrument, is about 1 m [26]; moreover, it was experimentally verified that the silicone cladding fibers produced a “dead zone” of about 20 m.

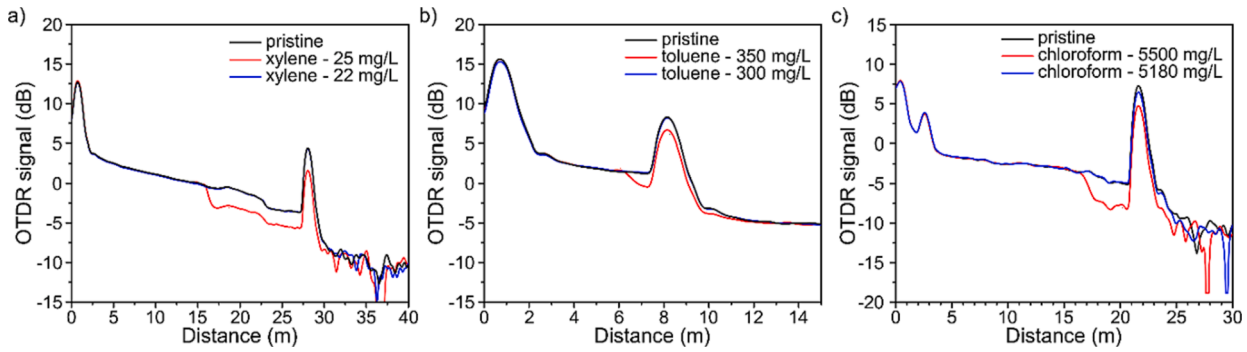

Fig. 9. OTDR traces obtained from the detection limit tests for aqueous solutions of (a) xylene, (b) toluene, and (c) chloroform. Each graph reports the curves of the pristine fiber, i.e., before immersion (black), the same fiber immersed in a solution at the limit concentration (red), and at a lower concentration than the detection limit (blue). The immersion points were at 17, 6.5, and 16 m for the tests (a), (b) and (c), respectively.

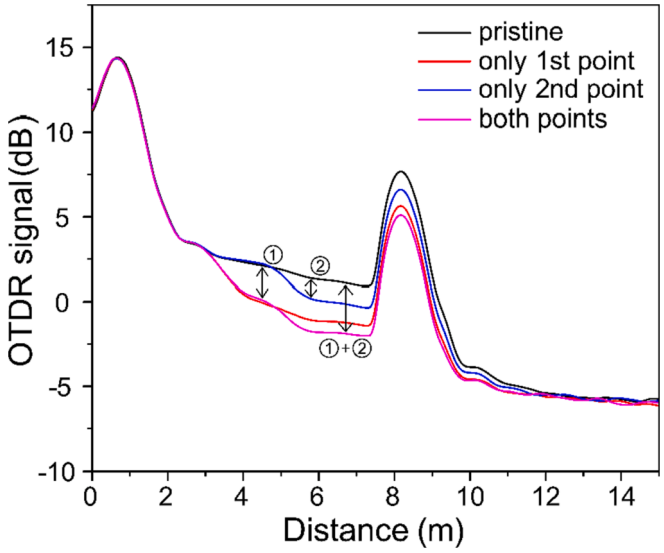

Fig. 10. Experimental demonstration of multiple leaks detection. The sensing fiber is exposed to dichloromethane at a first location (~3 m), and at a second location (~5 m), in two separate experiments. In a third test, the leakage is simulated at both locations, producing a double drop step in the OTDR trace. Therefore, the two leakage events appear detectable.

In order to detect scattering events with an accuracy in the order of a cm (as it may be required for the monitoring of some tanks) and without any "dead zone", OFDR measurements were also conducted with pure solvents. Fig. 11 shows the traces for tests performed using water, xylene, toluene, and chloroform. In this case, the event related to solvent absorption appears as a reflection peak, due to the mechanical stress associated with swelling. Immediate and reversible responses were observed during the tests conducted with the OFDR, along with a remarkable spatial resolution. The legend reports the position of the exposure, with respect to the input of the instrument, as measured by a ruler. Exposure occurred at 1.6 m for xylene, at 3.1 m for toluene, and 2.5 m for chloroform. The leakage events were detected at corresponding positions of 1.71, 2.96 and 2.60 m, respectively, hence with a maximum error of 14 cm, which can be considered as the upper accuracy bound when detecting the location of leakages. It should be pointed out that the instrument was used to sample Rayleigh backscattering at a resolution of 0.1 mm. Therefore, the discrepancy may be ascribed to two reasons. First, the instrument was devised to work with single-mode fibers, whereas the fiber here is highly multimode and each mode travels along the fiber at a different velocity, thereby producing uncertainties about the time (and equivalent position) at which a reflection event is detected. A further source of uncertainty may be due to the diffusion of the initial drop of HC along the fiber: the tests were performed by wetting 2 cm of sensing fiber, but the width of the corresponding events was 4 to 6 cm, as observable in Fig. 11b-d.

4. Conclusion and outlook

A distributed sensing system for hydrocarbon (HC) detection, based on silicone cladding optical fibers with a reduced cladding thickness and interrogation by means of a multimode Optical Time Domain Reflectometer (OTDR) has been investigated. The silicone used to produce the fiber cladding was characterized by gravimetric measurements during the diffusion of some representative HCs and water, and it was shown that this could be used as selective cladding material with suitable optical properties. The diffusion coefficients for the different HCs were estimated, through a simplified 1-D model, to calculate the diffusion time through a small cladding thickness (12.5 to 32.5 μm) that would produce an optical fiber with dimensions that matched those required for commercial OTDRs. Three different silicone cladding multimode optical fibers were fabricated and successfully tested with a multimode OTDR working at 850 nm. In order to have an easy, low loss and repeatable connection with the instrument, a fusion splicing recipe was developed to connectorize the sensing fiber with the standard connectors used in telecommunications. The distributed sensors produced in this way exhibited a good sensitivity to HCs that have a high refractive index, such as xylene, toluene and chloroform, but were insensitive to exposure to pure water. Their time response was constrained to 10 s by the OTDR acquisition parameters, but the fiber itself allowed a response quicker than 1 s to be obtained. The sensing system also demonstrated the ability to detect HCs in a water solution. Optical Frequency Domain Reflectometry (OFDR) proved to be a viable alternative to OTDR. With this instrument, HC detection appears as a reflection event. The tests with OFDR showed that the location of HC exposure is determined with an accuracy of 14 cm, and an almost instantaneous response. However, it should be considered that an OFDR instrument is about 6 to 10 times more expensive than an OTDR. Therefore, OFDR interrogation may be suitable for small infrastructures in which even small leakages have to be accurately detected to enable a prompt and efficient intervention. In the tested configuration, both OTDR and OFDR were able to interrogate fibers up to a distance of 2 km, but the investigations here reported were limited to lengths below 100 m, since the silicone cladding fibers were non-optimized prototypes that exhibited certain defects (bubbles in the glass, slight variation of the dimensions). However, some engineering in the fiber fabrication could clearly improve the performance, in terms of interrogation length. Moreover, in order to make the system suitable for in-situ testing, the sensing fiber would need to be mechanically protected. This could be achieved by coiling the fiber on a support cable or by embedding it in a woven shield.

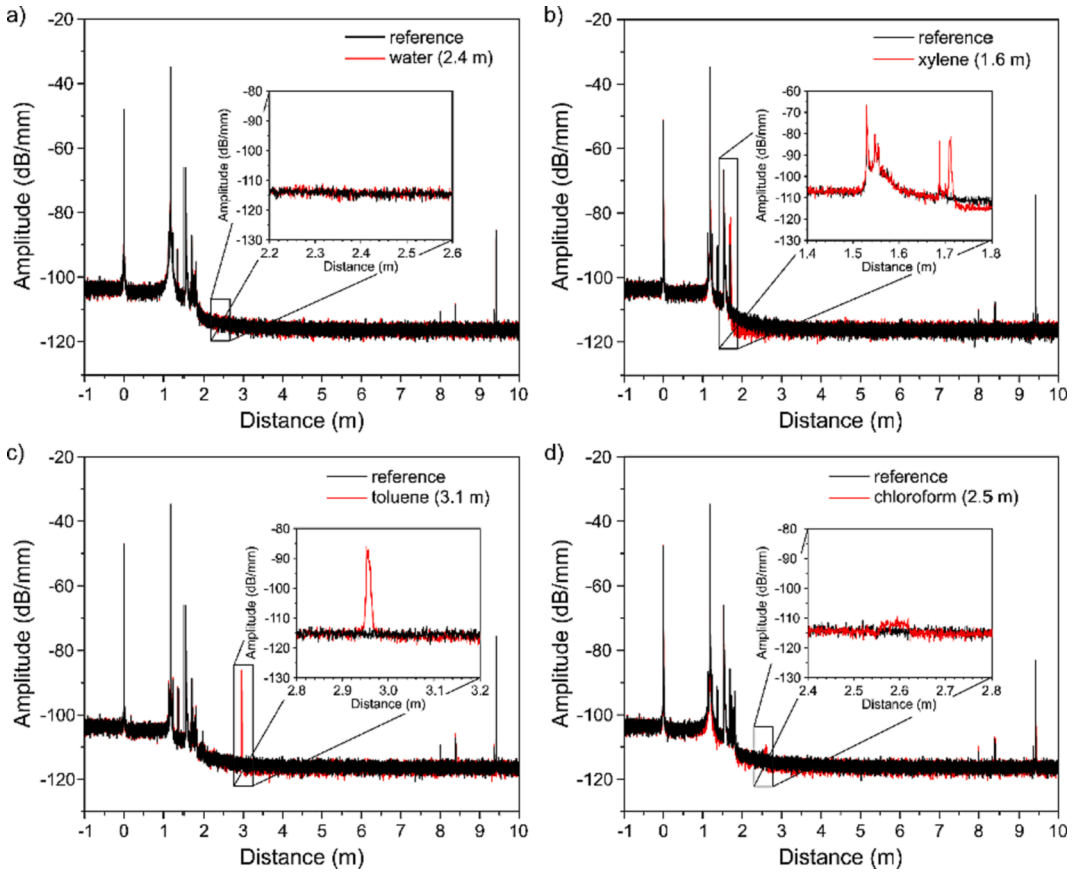

Fig. 11. OFDR measurements of a silicone cladding fiber exposed for a length of 2 cm in (a) water, (b) xylene, (c) toluene, and (d) chloroform. The insets depict a zoom of the reflection peak corresponding to the exposed section. The width of the peak represents the resolution. The value in brackets is the position of the exposure, as measured with a ruler.

Funding

This research was supported by Compagnia di San Paolo, through LINKS foundation and LIFTT society, under the grant "PoC cut-off2 2020".

The experimental activity was also supported by Politecnico di Torino through the competence center PhotoNext and by Piedmont Region through the project "FIP: Fotonica in Piemonte".

Declaration of Competing Interest

The authors declare that they have no known competing financial interests or personal relationships that could have appeared to influence the work reported in this paper.

Data availability

Data will be made available on request.

References

[1] Statista, Petrochemical industry worldwide. https://www.statista.com/study/70670/global-petrochemical-industry/, 2022 (accessed 02 September 2022).
[2] Fossil fuels, Few oil pipeline spills detected by much-touted technology, https://insideclimatenews.org/news/19092012/few-oil-pipeline-spills-detected-much-touted-technology/, 2022 (accessed 02 September 2022).
[3] M.A. Adegboye, W.-K. Fung, A. Karnik, Recent advances in pipeline monitoring and oil leakage detection technologies: principles and approaches, Sensors. 19 (2019) 2548, https://doi.org/10.3390/s19112548.
[4] O.P. Jiménez, R.M.P. Pastor, O.E. Segovia, S. Del Reino Querencia, Exploring petroleum hydrocarbons in groundwater by double solid phase extraction coupled to gas chromatography–flame ionization detector, Talanta 131 (2015) 315–324, https://doi.org/10.1016/j.talanta.2014.06.042.
[5] S. Fu, J. Fan, Y. Hashi, Z. Chen, Determination of polycyclic aromatic hydrocarbons in water samples using online microextraction by packed sorbent coupled with gas chromatography–mass spectrometry, Talanta 94 (2012) 152–157, https://doi.org/10.1016/j.talanta.2012.03.010.
[6] R. Lu, B. Mizaikoff, W.-W. Li, C. Qian, A. Katzir, Y. Raichlin, G.-P. Sheng, H.-Q. Yu, Determination of chlorinated hydrocarbons in water using highly sensitive mid-infrared sensor technology, Sci. Rep. 3 (2013) 2525, https://doi.org/10.1038/srep02525.
[7] B.L. Wittkamp, S.B. Hawthorne, D.C. Tilotta, Determination of aromatic compounds in water by solid phase microextraction and ultraviolet absorption spectroscopy. 1. Methodology, Anal. Chem. 69 (1997) 1197–1203, https://doi.org/10.1021/ac960761d.
[8] O. Péron, E. Rinnert, M. Lehaitre, P. Crassous, C. Compère, Detection of polycyclic aromatic hydrocarbon (PAH) compounds in artificial sea-water using surface-enhanced Raman scattering (SERS), Talanta 79 (2009) 199–204, https://doi.org/10.1016/j.talanta.2009.03.043.
[9] R.J. Law, Hydrocarbon concentrations in water and sediments from UK marine waters, determined by fluorescence spectroscopy, Mar. Pollut. Bull. 12 (1981) 153–157, https://doi.org/10.1016/0025-326X(81)90226-5.
[10] R. Risi, Performing reliable early leak detection on storage tank terminals: retrofitting of existing facilities and new buildings, J. Mater. Sci. Eng. B. 8 (2018) 188–194, https://doi.org/10.17265/2161-6221/2018.9-10.002.
[11] R. Falate, R.C. Kamikawachi, M. Müller, H.J. Kalinowski, J.L. Fabris, Fiber optic sensors for hydrocarbon detection, Sens. Actuators, B Chem. 105 (2005) 430–436, https://doi.org/10.1016/j.snb.2004.06.033.
[12] A. Güemes, A. Fernández-López, B. Soller, Optical fiber distributed sensing - physical principles and applications, Struct. Health Monit. 9 (2010) 233–245, https://doi.org/10.1177/1475921710365263.
[13] A. MacLean, C. Moran, W. Johnstone, B. Culshaw, D. Marsh, P. Parker, Detection of hydrocarbon fuel spills using a distributed fibre optic sensor, Sens. Actuators, A Phys. 109 (2003) 60–67, https://doi.org/10.1016/j.sna.2003.09.007.
[14] C. Totland, P.J. Thomas, I.F. Størdal, E. Eek, A fully distributed fibre optic sensor for the detection of liquid hydrocarbons, IEEE Sens. J. 21 (2021) 7631–7637, https://doi.org/10.1109/JSEN.2020.3047549.
[15] S.-C. Huang, W.-W. Lin, M.-T. Tsai, M.-H. Chen, Fiber optic in-line distributed sensor for detection and localization of the pipeline leaks, Sens. Actuators, A Phys. 135 (2007) 570–579, https://doi.org/10.1016/J.SNA.2006.10.010.
[16] F. Tanimola, D. Hill, Distributed fibre optic sensors for pipeline protection, J. Nat. Gas Sci. Eng. 1 (2009) 134–143, https://doi.org/10.1016/j.jngse.2009.08.002.

[17] M. Nikles, 2009. Long-distance fiber optic sensing solutions for pipeline leakage, intrusion, and ground movement detection. Proc. SPIE 7316, Fiber Optic Sensors and Applications VI 7316, 731602. Doi: 10.1117/12.818021.
[18] P. Stajanca, S. Chruscicki, T. Homann, S. Seifert, D. Schmidt, A. Habib, Detection of leak-induced pipeline vibrations using fiber—optic distributed acoustic sensing, Sensors. 18 (2018) 2841, https://doi.org/10.3390/s18092841.
[19] Development Operations & Tecnology Department. ENI S.p.A., Private communication, 2018.
[20] E. Sensfelder, J. Bürck, H.-J. Ache, Characterization of a fiber-optic system for the distributed measurement of leakages in tanks and pipelines, Appl. Spectrosc. 52 (1998) 1283–1298, https://doi.org/10.1366/0003702981942799.
[21] J. Buerck, S. Roth, K. Kraemer, H. Mathieu, OTDR fiber-optical chemical sensor system for detection and location of hydrocarbon leakage, J. Hazard. Mater. 102 (2003) 13–28, https://doi.org/10.1016/S0304-3894(03)00199-7.
[22] J.M. Buerck, B.H. Vogel, S. Roth, S. Ebrahimi, K. Kraemer, 2004. Distributed fiber optical HC leakage and pH sensing techniques for implementation into smart structures. Proc. SPIE 5384, Smart Structures and Materials 2004: Smart Sensor Technology and Measurement Systems 5384. Doi: 10.1117/12.538240.
[23] RP Photonics Encyclopedia – Optical time-domain reflectometers. https://www.rp-photonics.com/optical_time_domain_reflectometers.html (accessed 20 March 2022).
[24] D. Derickson, Fiber Optic Test and Measurement, first ed., Prentice Hall, Hoboken, 1998.
[25] Z. Ding, C. Wang, K. Liu, J. Jiang, D. Yang, G. Pan, Z. Pu, T. Liu, Distributed optical fiber sensors based on optical frequency domain reflectometry: a review, Sensors. 18 (2018) 1072, https://doi.org/10.3390/s18041072.
[26] Refractive index of SiO2 (Silicon dioxide, Silica, Quartz) - Malitson Available online: https://refractiveindex.info/?shelf=main&book=SiO2&page=Malitson (accessed 09 March 2022).
[27] C. Marro Bellot, G. De Leo, H. Zhang, A. Kernin, C. Scarponi, M. Sangermano, M. Olivero, E. Bilotti, M. Salvo, Dual in-situ water diffusion monitoring of GFRPs based on optical fibres and CNTs, J. Compos. Sci. 4 (2020) 97, https://doi.org/10.3390/jcs4030097.